*Published online 19 December 2016* *Nucleic Acids Research, 2017, Vol. 45, No. 5* **2585–2599**
*doi: 10.1093/nar/gkw1262*

# Microhomology-mediated end joining is activated in irradiated human cells due to phosphorylation-dependent formation of the XRCC1 repair complex

**Arijit Dutta[1,2], Bradley Eckelmann[1,3], Sanjay Adhikari[4], Kazi Mokim Ahmed[1], Shiladitya Sengupta[1,5], Arvind Pandey[1], Pavana M. Hegde[1], Miaw-Sheue Tsai[6], John A. Tainer[6,7], Michael Weinfeld[8], Muralidhar L. Hegde[1,5,9] and Sankar Mitra[1,2,3,5,*]**

[1]Department of Radiation Oncology, Houston Methodist Research Institute, Houston, TX 77030, USA, [2]Department of Biochemistry and Molecular Biology, University of Texas Medical Branch (UTMB), Galveston, TX 77555, USA, [3]Texas A&M Health Science Center, College of Medicine, Bryan, TX 77807, USA, [4]EntroGen, Inc., Woodland Hills, CA 91367, USA, [5]Weill Cornell Medical College, New York, NY 10065, USA, [6]Department of Cell and Molecular Biology, Lawrence Berkeley National Laboratory (LBNL), Berkeley, CA 94720, USA, [7]Department of Molecular and Cellular Oncology, The University of Texas MD Anderson Cancer Center, Houston, TX 77030, USA, [8]Department of Oncology, University of Alberta, Cross Cancer Institute, Edmonton, Alberta T6G 1Z2, Canada and [9]Houston Methodist Neurological Institute, Houston, TX 77030, USA

Received May 17, 2016; Revised December 01, 2016; Editorial Decision December 02, 2016; Accepted December 15, 2016

## ABSTRACT

**Microhomology-mediated end joining (MMEJ), an error-prone pathway for DNA double-strand break (DSB) repair, is implicated in genomic rearrangement and oncogenic transformation; however, its contribution to repair of radiation-induced DSBs has not been characterized. We used recircularization of a linearized plasmid with 3′-P-blocked termini, mimicking those at X-ray-induced strand breaks, to recapitulate DSB repair via MMEJ or nonhomologous end-joining (NHEJ). Sequence analysis of the circularized plasmids allowed measurement of relative activity of MMEJ versus NHEJ. While we predictably observed NHEJ to be the predominant pathway for DSB repair in our assay, MMEJ was significantly enhanced in preirradiated cells, independent of their radiation-induced arrest in the G2/M phase. MMEJ activation was dependent on XRCC1 phosphorylation by casein kinase 2 (CK2), enhancing XRCC1's interaction with the end resection enzymes MRE11 and CtIP. Both endonuclease and exonuclease activities of MRE11 were required for MMEJ, as has been observed for homology-directed DSB repair (HDR). Furthermore, the XRCC1 co-immunoprecipitate complex (IP) displayed MMEJ activity *in vitro*, which was significantly elevated after irradiation. Our studies thus suggest that radiation-mediated enhancement of MMEJ in cells surviving radiation therapy may contribute to their radioresistance and could be therapeutically targeted.**

## INTRODUCTION

About half of all cancer patients are treated with ionizing radiation (IR), either alone or in combination with surgery and/or chemotherapy (1). However, invariable development of resistance to radiotherapy in recurrent cancers warrants comprehensive understanding of the repair of IR-induced DNA damage, which promotes tumor cell survival. IR induces clustered damage in the genome, including highly cytotoxic double-strand breaks (DSBs), together with an excess of closely spaced single-strand breaks (SSBs), abasic (AP) sites and oxidized bases (2). In dividing cells, DSBs can be repaired accurately in the S/G2 phase via homology-dependent repair (HDR) which requires resection at the 5′ DSB termini to generate 3′ overhangs, followed by invasion of the homologous sequence in the undamaged sister chromatid (3). However, NHEJ, which involves ligation of blunt ends, is the predominant pathway for DSB repair (DSBR), independent of cell cycle phase (4). Although NHEJ can be error-prone at complex DSBs (5) as a result of end resection and/or gap filling prior to ligation (6), the binding of Ku limits end resection at DSB ends, preventing

*To whom correspondence should be addressed. Tel: +1 713 441 7148; Fax: +1 713 790 3755; Email: smitra2@houstonmethodist.org

significant loss of nucleotides (7). A recently characterized, highly error-prone DSBR process variously named backup NHEJ, alternative NHEJ, or alternative end joining (Alt-EJ), does not require NHEJ proteins but utilizes the base excision/single-strand break repair (BER/SSBR) proteins including poly(ADP-ribose) polymerase 1 (PARP1), X-ray repair cross-complementing protein 1 (XRCC1) and DNA ligase 1 or 3 (LIG1/3) for joining the DSB termini (8–10). Significant diversity in Alt-EJ has been observed, with several sub-pathways differing in their requirement for preexisting or *de novo* microhomology (11), while a few reports have described microhomology-independent processes for Alt-EJ (12,13).

Microhomology-mediated Alt-EJ (MMEJ) carries out DSB joining via annealing of short microhomology sequences (5–25 bases) to the complementary strand spanning the break site (11). The consensus requirement for MMEJ is the initial resection of DSB ends by MRE11/RAD50/NBS1 (MRN) and CtIP, analogous to that observed in HDR, in order to generate a 3′ single-stranded DNA (ssDNA) overhang that helps search for microhomology sequences across the DSB (14). After annealing of the microhomology sequences, any resulting flap segments are removed by the endonuclease activity of CtIP or flap endonuclease 1 (FEN-1), followed by gap-filling in both strands by a DNA polymerase, such as DNA polymerase θ or λ (Polθ/λ), and finally ligation of the nicks by LIG1/3 (15). However, how these steps are regulated is not understood. In any event, MMEJ results in loss of one microhomology sequence and the intervening region, which leads to deletions of variable size. MMEJ is mechanistically similar to an HDR process named single-strand annealing (SSA); however, the latter involves annealing of DSB termini over large homology regions (>30 bases) mediated by Rad52 (11). MMEJ, active in both normal and cancer cells (8), could serve as a backup pathway to NHEJ (16). However, recent studies have suggested that it could be a dedicated pathway in cancer cells, particularly those with deficiencies in HDR activity (17,18). Whole-genome sequence data from large cohorts of cancer patients has suggested a significant contribution of MMEJ to the genomic instability in cancer cells, via deletion, insertion, inversion, and complex structural changes (19,20).

In the present study, we investigated the contribution of MMEJ to repair of IR-induced DSBs. Strand breaks generated by IR have non-ligatable termini containing 3′-phosphate (P) and/or 3′-phosphoglycolate (21), which need to be removed to generate the 3′-OH terminus required for repair synthesis and ligation (22). Incidentally, the proportion of 3′-P termini at IR-induced strand breaks in synthetic oligonucleotides increases under hypoxic and anoxic conditions (23). To assess the relative contribution of MMEJ versus NHEJ at IR-induced DSBs, we developed an *in cell* assay based on circularization of a linearized GFP reporter plasmid containing 3′-P termini, followed by sequence analysis of the repaired joints. After documenting that *in cell* circularization of this novel substrate recapitulated the requirements for NHEJ and MMEJ in the cellular genome, we observed that MMEJ activity is low relative to NHEJ in untreated cells, as expected. However, MMEJ activity was significantly enhanced after radiation treatment. We then focused on the scaffold protein XRCC1, which interacts with both SSBR proteins and MRN, all of which are recruited at IR-induced clustered damage sites. We tested the hypothesis that XRCC1, via phosphorylation by casein kinase 2 (CK2), forms a repair-competent complex to carry out MMEJ. Finally, our observation that the XRCC1-IP can perform MMEJ *in vitro,* similar to what our group observed previously with BER complexes (24), could allow us to identify undiscovered factors involved in MMEJ.

## MATERIALS AND METHODS

### Cell culture and X-ray irradiation

All *in cell* and *in vitro* repair assays were performed with U2OS and A549 cells. Stable shRNA-mediated PNKP-downregulated A549-shPNKP cells were described earlier (25). All cell lines were cultured in Dulbecco's modified Eagle medium (DMEM; high-glucose; Gibco-BRL) supplemented with 10% fetal calf serum (Sigma) and 100 U/ml penicillin and 100 μg/ml streptomycin (Gibco-BRL). A549-shPNKP cells were grown in DMEM selection medium with 300 μg/ml Geneticin sulfate (Thermo Fisher). The cells were irradiated using a Rad Source RS 2000 X-ray irradiator (Rad Source Technologies, Inc., GA, USA).

### Inhibitors

Cells were pretreated with 10 μM NU7441 (Tocris) for 1 h to inhibit DNA-PK, 50 μM CX-4945 or silmitasertib (Abcam) for 2 h to inhibit CK2, or 100 μM Mirin (Sigma) for 1 h to inhibit MRE11 exonuclease activity. During *in vitro* MMEJ assays (as described below), XRCC1-IP was incubated with either 100 μM Mirin or 100 μM MRE11 endonuclease inhibitor, PFM03 (26), for 15 min.

### Generation of linearized plasmid substrate pNS with 3′-P termini

In order to generate a DSB containing 3′-P termini, we introduced two closely spaced uracil (U) residues, 2-nt apart on opposite strands, in the pEGFPN1 plasmid backbone. Excision of U by uracil DNA glycosylase (UDG), followed by strand scission at the resulting AP sites by FapyG DNA glycosylase (Fpg) generated 3′-P and 5′-P termini (Figure 1A) (27). However, direct ligation of U-containing duplex with oligonucleotide into a pEGFPN1 backbone gave a very low yield of the final product which was not sufficient for performing the repair assays (not shown). To increase the yield, we adopted a two-step nicking methodology where U-containing oligonucleotides were sequentially introduced at the target site, with the complementary strand, providing a template for annealing, followed by nick sealing by T4 DNA ligase (Supplementary Figure S1 and Supplemental Materials and Methods). The nicking endonucleases Nt.BbvCI and Nb.BbvCI (NEB) are neoisoschizomers that recognize the same heptanucleotide sequence, 5′-CCTCAGC-3′, but create nicks on complementary strands. At first, a duplex oligonucleotide NT2NB2 (41 nts) containing two CCTCAGC sequence flanking the target site was introduced between EcoR1 and

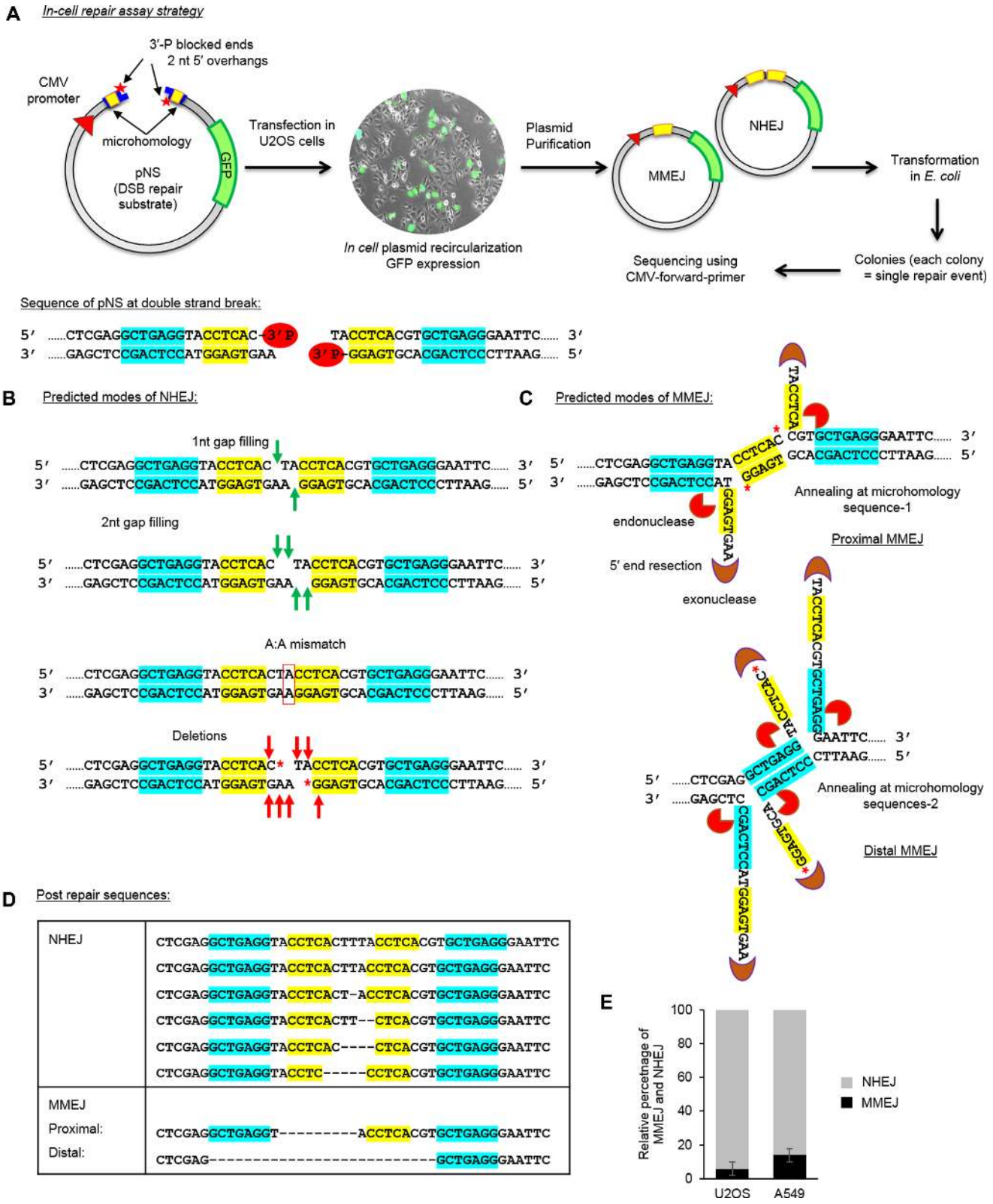


**Figure 1.** Development of an *in cell* DSB repair assay with a linearized plasmid substrate that mimics an X-ray induced DSB. (**A**) Schematic representation of the *in cell* repair assay with pNS; below is the sequence of pNS containing the DSB. The 5-nt sequences highlighted in yellow are microhomology sequence-1, the 7-nt nicking endonuclease sequences (see Supplementary Figure S1) highlighted in cyan are microhomology sequence-2, and 3′-P nonligatable termini are highlighted in red circles. (**B**) Predicted modes of NHEJ, either 1 or 2-nt gap-filling, post-DSB end-joining A:A mismatch repair, or deletion of terminal bases by exonucleases to generate flush ends. (**C**) Predicted modes of MMEJ, the 3′ overhangs could be annealed through either microhomology sequence-1 or -2 with exo/endonucleolytic processing of the intervening sequences. (**D**) Sequences at repaired joints of circularized pNS after *in cell* repair. (**E**) Relative percentage of MMEJ/NHEJ repair of pNS in U2OS and A549 cells.

Xho1 within the pEGFPN1 multiple cloning site (Supplementary Figure S1A and B). This modified pEGFPN1 vector, named pNt.Nb, was amplified by a plasmid maxiprep procedure and was used to generate the final linearized plasmid substrate. 100 μg pNt.Nb was incubated with Nt.BbvCI, followed by removal of the enzyme by column purification with the Qiagen PCR purification kit. The nicked fragment was then dissociated from the plasmid by partial denaturation at 65°C for 10 min, followed by annealing with 100-fold molar excess of the first U containing oligonucleotide, NtU. The intermediate was ligated overnight (15 h) at 16°C with T4 DNA ligase (NEB), followed by column purification of the ligated plasmid, named pNtU.Nb. Next, pNtU.Nb was treated with Nb.BbvCI, which nicked the strand opposite to the now U-containing strand. This was followed by similar introduction of the second U-containing oligonucleotide, NbU. The final ligation product, pNtU.NbU, with U on opposite strands was gel purified and then treated with UDG in 1X UDG buffer, followed by addition of Fpg and 1X NEB buffer 1. The linearized plasmid, pNS was gel purified twice to remove contamination of the nicked fraction. All intermediate products were checked for purity by agarose (1%) gel electrophoresis (Supplementary Figure S1B). pNS was checked for purity using a transformation based assay. One nanogram pNS or serially diluted circular pEGFPN1 (1000, 10, 1 and 0.1 pg) was used to transform *E coli* DH5α competent cells and plated in kanamycin (50 μg/ml)-containing LB agar in triplicate. The number of colonies observed with 1 ng pNS was similar to that with 1 pg circular pEGFPN1. We thus inferred that the pNS preparation contained <1 pg circular pEGFPN1, indicating its >99.9% purity (Supplementary Figure S1C).

### *In-cell* plasmid circularization assay

U2OS or A549 cells grown in 60 mm plates (50% confluent) were transfected with 100 ng pNS, the repair substrate, using Lipofectamine 2000 and incubated overnight (15 h). The cells were then checked for GFP expression and plasmids were isolated using the Qiagen plasmid miniprep kit (28). It should be noted that GFP reporter was used only to confirm transfection efficiency and circularization of the linearized plasmid substrate in the human cells via DSB repair. XL10-gold ultracompetent *E. coli* (Agilent) were transformed with 5 μl plasmid solution following the manufacturer's protocol. Forty to fifty colonies were randomly selected for sequencing using the CMV-F primer by Genewiz, Inc. (South Plainfield, NJ, USA). The sequences of individual plasmid clones surrounding the rejoined break site were analyzed by using the multiple sequence alignment tool, Multalin (INRA). Sequences with insertions/deletions of 1–4 nts at the DSB site were scored as NHEJ products, while the plasmids with deletion of one of the 5 nt microhomology sequences, CCTCA, were scored as products of MMEJ. Notably, two nicking endonuclease sites (GCTGAGG; highlighted blue, Figure 1A) introduced in the plasmid backbone flanking the DSB site could also serve as microhomology sequences, and in some of the repaired products, one of these sequences was additionally deleted. We scored such sequences as products of MMEJ. Non-specific extended deletions (>10 nt) at the 3′or 5′ end of the DSB were not taken into account while plotting MMEJ versus NHEJ. The relative percentages of MMEJ/NHEJ sequences were plotted and the statistical analysis was performed using a two-tailed Fisher's exact test.

### Co-immunoprecipitation and *in vitro* MMEJ assay

Exponentially growing U2OS cells transiently expressing XRCC1-FLAG were treated with inhibitors/siRNAs as indicated and irradiated with X-rays (3 Gy). After 1 h, the irradiated and control cells were harvested for preparation of nuclear extracts. XRCC1-FLAG IP was isolated by incubating the nuclear extract with FLAG-M2 agarose beads for 2 h at 4°C. The beads were directly incubated for 30 min with 5 ng pNS in a reaction buffer containing 2 mM $MgCl_2$, 60 mM NaCl, 50 mM HEPES, 2 mM DTT, 1 mM ATP, 1 mM dNTPs, and 50 μg/ml bovine serum albumin (BSA) with gentle shaking at 30°C. This was followed by the addition of 14 ng XRCC1/LIG3α recombinant protein complex into the reaction mix for further incubation for 15 h at 16°C. After removal of the beads by low speed centrifugation, 5 μl supernatant was used for transformation of XL10-gold ultracompetent *E. coli* cells (Agilent Technologies). The separated beads were also eluted with 4× LDS loading buffer for Western analysis. The colonies in each plate were counted and submitted for sequence analysis using the CMV-F primer (Genewiz Inc.) similar to that used in the *in cell* assay. We observed 2–4 colonies in the control IP plates which were presumably due to transformation of linearized plasmid in E. *coli* at a very low frequency (4–8 cfu/ng linear DNA compared to $5 \times 10^6$ cfu/ng circular DNA). Therefore, we normalized the data in all experimental sets to the control IP.

For details regarding plasmids and siRNAs, antibodies, preparation of total cell and nuclear extracts, proximity ligation assay (PLA), immuno-staining, clonogenic cell survival, γH2AX foci analysis, fluorescence-activated cell sorting and gel filtration analysis, see Supplementary Information.

## RESULTS

### *In cell* DSB repair assay recapitulates repair of blocked DSB termini induced by radiation

The mechanisms of DSBR in the mammalian genome are commonly investigated through generation of site-specific DSBs by an ectopic meganuclease such as I-*Sce*I (29). Although this strategy can quantitatively characterize HDR versus NHEJ at specific genomic loci, the induced DSBs do not resemble the complex strand breaks induced by ionizing radiation, which include SSBs, oxidized bases, and DSBs with non-ligatable termini (30). To explore how radiation-induced DSBs are repaired in the genome, we used circularization of a reporter plasmid, linearized with nonligatable 3′-P termini, as a model system for analyzing DSB repair via NHEJ or MMEJ. We followed the repair, i.e. circularization of the linearized GFP reporter plasmid, pNS, in transfected human cells from which the plasmid population was recovered and screened in *E. coli*. The plasmid molecules

circularized in the human cell produced kanamycin resistant colonies based on expression of the drug resistance gene in the plasmid (pEGFPN1). Noncircularized plasmid molecules recovered from the human cells could not be circularized in *E. coli* because these are promptly degraded by the RecB/C nuclease. Linearized plasmid was shown to have $> 10^3$-fold lower transformation efficiency than the circular plasmid in wild-type *E. coli* used in our experiments, supporting previous observations (31). To ensure that we eliminated any chance of recovering drug resistant *E.coli* colonies resulting from plasmid recircularization in the *E. coli,* we treated the plasmid extracted from transfected human cells with lambda exonuclease (NEB) to remove any linear plasmids. We observed no significant difference in the transformation efficiency or in the relative products of NHEJ versus MMEJ in untreated vs. lambda exonuclease-treated plasmid extracts, as we had expected (Supplementary Figure S2). Finally, DSB repair via HDR was precluded because the plasmids lack the ability to replicate in human cells. Thus, each bacterial colony represented an individual DSB repair event in the human cell. Subsequent sequence analysis of the rejoined region in individual plasmids allowed us to evaluate the relative contribution of NHEJ and MMEJ to the repair of the DSB in pNS.

In order to quantitate the relative contribution of MMEJ versus NHEJ, we introduced a pair of 5 nt long microhomology sequences flanking the DSB (Figure 1A), following the current consensus on the requirement for MMEJ, as has been characterized by both *in vitro* and chromatin-based DSB repair assays in human and yeast cells (8,32,33). We transfected human osteosarcoma U2OS cells or human lung carcinoma A549 cells at 70–80% confluency with linearized pNS, which expresses GFP only if circularized via DSB repair (end joining). Although GFP expression was observed as early as 6 h after transfection (Figure 1A), we routinely harvested cells after overnight incubation (15 h) of the transfected cells before extracting the plasmid for transforming *E. coli.* At least 40 kanamycin-resistant colonies were randomly selected for sequencing using a CMV-F primer. NHEJ requires blunt termini with 5′-P and 3′-OH, generated either by removal of the 3′-P termini by PNKP (34), exonucleolytic degradation of a few terminal bases, or gap-filling synthesis, which leads to either error-free repair or that with a small deletion/insertion (Figure 1B). On the other hand, MMEJ of our plasmid substrate would involve annealing at the microhomology sequence, resulting in a larger deletion with the loss of one microhomology sequence (Figure 1C). We observed long non-specific deletions (>10 nt) in a small number of plasmid molecules, which were ignored because of their likely formation due to non-specific exo/endonucleolytic degradation at the DSB termini. Thus, the molecules with only a 1–3 nt insertion or 1–10 nt deletion were scored as products of NHEJ, while those with a deletion of one microhomology sequence (including the intervening sequence) were counted as products of MMEJ (Figure 1D). *In cell* repair of pNS showed that NHEJ was the predominant contributor to repair of pNS in both U2OS and A549 cells, while a small fraction of repair events (14% in A549 and 8% in U2OS) were of the MMEJ type (Figure 1E). These results are in general agreement with the published literature that NHEJ is the predominant contributor to DSB repair in the human cell genome relative to MMEJ (15).

### Inhibition of 3′-P removal at DSB termini increases MMEJ frequency

Because ligation requires removal of the 3′-P at DNA termini by PNKP (35), we tested the effect of PNKP deficiency on MMEJ. We analyzed end joining of pNS in A549 cells in which PNKP was depleted via stable expression of its shRNA (Figure 2A) (25). The frequency of MMEJ in PNKP-depleted cells was 3-fold higher compared to that in the wild type (WT) cells, which was reversed by ectopic expression of WT-PNKP but not by the phosphatase-inactive mutant (Figure 2A and B). These results strongly suggest that NHEJ involves 3′-P removal by PNKP, as reported earlier (34), and that its deficiency promotes MMEJ-mediated DSB repair. Although it has been suggested that PNKP promotes MMEJ *in vitro* via its interaction with PARP1-XRCC1/Ligase 3 (LIG3) (12), our results indicate that it is dispensable during *in cell* MMEJ that utilizes microhomology.

### MMEJ is enhanced in preirradiated cancer cells

We then asked whether MMEJ and NHEJ are affected in cells by radiation-induced activation of the DNA damage response signaling. We irradiated A549 and U2OS cells with various doses of X-rays immediately before transfection with pNS, and then analyzed sequences of the repaired plasmids. The contribution of MMEJ relative to NHEJ was enhanced ∼5-fold after exposure to a 0.5 Gy or higher X-ray dose in both cell lines (Figure 2C and D, left four columns). These results are consistent with a previous report of induction of microhomology-mediated end joining in yeast and mammalian cells after irradiation, although its mechanism was not investigated (36). We also confirmed that the microhomology-dependent DSB end joining was not mediated by a variant NHEJ process, based on the result that MMEJ accounted for up to 95% of DSBR in U2OS cells when the cells were pretreated with the DNA-PK inhibitor NU7441 (Figure 2D, last column). Furthermore, induction of MMEJ in preirradiated cells was absent if any of the known MMEJ factors, namely, XRCC1, PARP1, MRE11 and CtIP, were either depleted by treatment with cognate siRNA or inhibited by specific inhibitors (Figure 2D and Supplementary Figure S3). To confirm that this observed increase in MMEJ after irradiation was not restricted to a particular genomic sequence, we performed the *in cell* repair assay with another linear plasmid substrate, pNX, which has incompatible ends and 3 different pairs of 4 nt-long microhomology regions (Supplementary Figure S4). Although the efficiency of DSBR was lower than that observed for pNS, MMEJ of pNX was observed only in preirradiated U2OS cells (Supplementary Figure S4). Moreover, there was a marked increase in deletions at DSB termini of pNX in preirradiated cells, indicating a greater extent of end resection.

Previous reports have suggested that MMEJ is a slow DSB repair process, which is stimulated during the G2 phase of the cell cycle (37,38). IR-induced genome damage

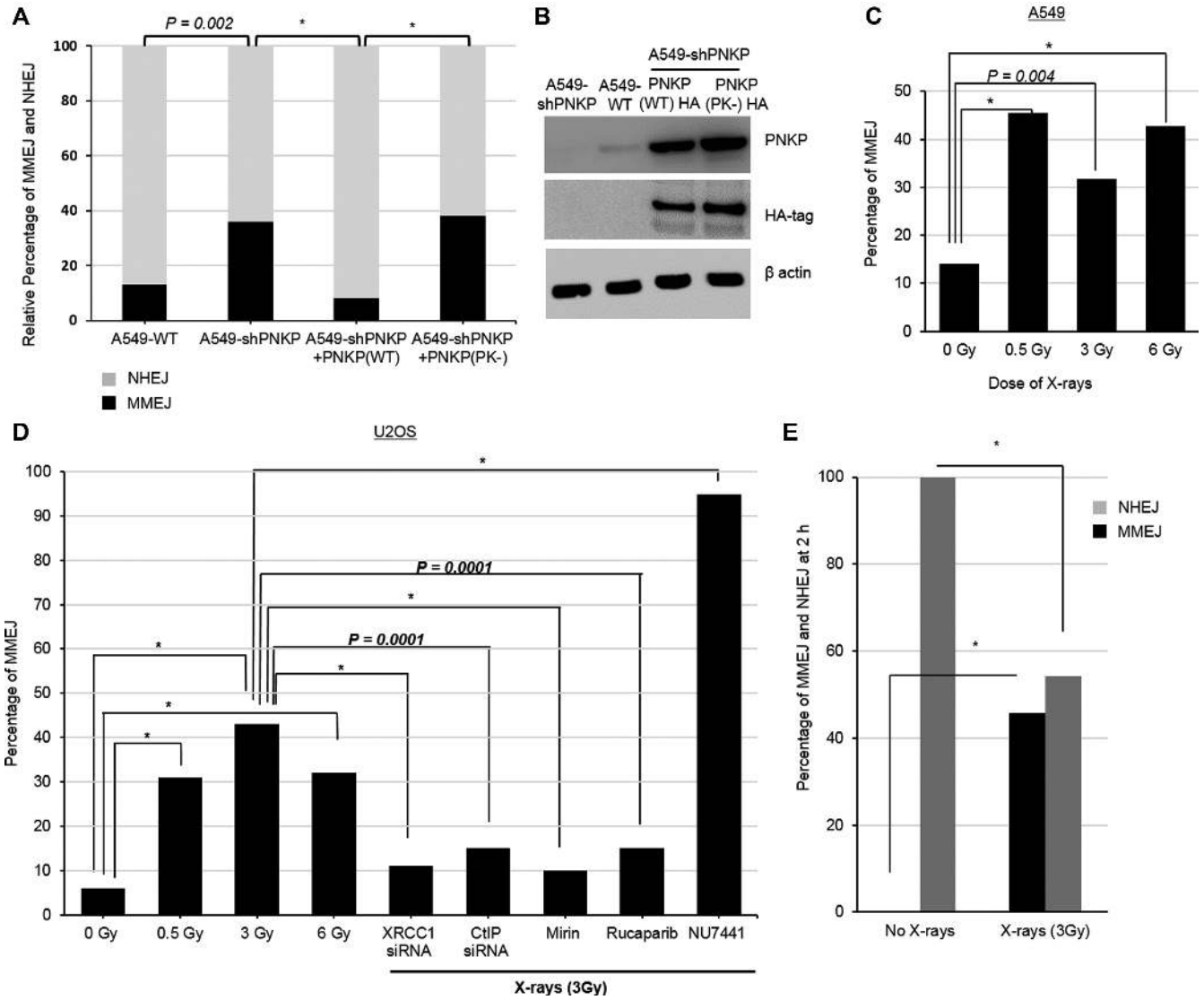


**Figure 2.** Relative percentage of MMEJ of blocked DSBs is enhanced in cancer cells after PNKP depletion and in preirradiated cells. (**A**) *In cell* repair of pNS in WT A549 cells, shRNA-mediated PNKP-depleted cells, or in endogenous PNKP-depleted cells with transient expression of HA-tagged PNKP-WT or PNKP-phosphatase/kinase inactive (PK-) mutant. (**B**) Western analysis of extracts from cells as in A. (**C**) *In cell* repair of pNS in control A549 cells and in cells preirradiated with various doses of X-rays, as indicated. (**D**) *In cell* repair of pNS in control U2OS cells and cells treated with different doses of X-rays, XRCC1 siRNA (100 nM, 72 h), CtIP siRNA (100 nM, 72 h), rucaparib (10 μM), mirin (100 μM), or NU7441 (10 μM), as indicated. (E) *In cell* repair of pNS in U2OS cells (± X-rays, 3 Gy) with plasmid extraction after 2 h (*$P < 0.0001$).

causes arrest of dividing human cells in the G2/M phase (39). We therefore tested if G2 arrest is responsible for enhancement of MMEJ in preirradiated cells, because our initial assay involved incubation of transfected cells for 15 h, by which time the cells should be arrested in the G2 phase. We confirmed this using fluorescence-activated cell sorting, which showed that U2OS cells were indeed arrested in the G2/M phase after irradiation (3 Gy) (Supplementary Figure S5). The fraction of cells in the G2 phase started to increase at 4 h post-irradiation; furthermore, ∼69% of the cells remained G2-arrested after 24 h. Based on these data, we then transfected preirradiated and untreated U2OS cells with pNS and harvested plasmid DNA 2 h later (before the onset of G2/M arrest) for transforming *E coli*. Sequence analysis of the repaired plasmids showed that MMEJ comprised 46% of DSB repair events at 2 h in post-irradiated cells, while it was completely absent in untreated cells for the same time period. These results are similar to our observations when we recovered plasmids after 15 h incubation (Figure 2E).

Because radiation-induced reactive oxygen species (ROS), such as OH• radicals, may have a common signaling process as $H_2O_2$ generated by glucose oxidase (GOx), we checked if GOx treatment similarly enhanced repair of pNS by MMEJ. Intriguingly, we did not observe activation of MMEJ in U2OS cells pretreated with either GOx or neocarzinostatin (Neo), which generates predominantly DSBs (Supplementary Figure S6A). We confirmed generation of SSBs and DSBs with the same doses of GOx and Neo, by

using alkaline and neutral comet assays and γH2AX foci formation assay (Supplementary Figure S6B–D).

### XRCC1 is recruited at DSBs for repair of X-ray-induced DSBs

Based on our observation that MMEJ is compromised in XRCC1-deficient U2OS cells, and also on published reports documenting the involvement of XRCC1 in MMEJ-mediated DSBR (8,9,40), we tested if XRCC1 localizes to X-ray-induced DSBs in the genome. Proximity ligation assay (PLA) for XRCC1 and the DSB marker γH2AX confirmed that XRCC1 was recruited at DSBs in irradiated cell nuclei (Figure 3A, upper panel; S13). Moreover, the number of PLA foci increased significantly after inhibition of DNA-PK with NU7441, suggesting that XRCC1's involvement in DSB repair is more pronounced when NHEJ is inhibited. Significant reduction in the number of PLA foci showing XRCC4-γH2AX co-localization in NU7441-pretreated cells confirmed NHEJ inhibition (Figure 3A, middle panel). The XRCC1-IgG PLA control exhibited no foci formation, confirming the signal specificities (Figure 3A, lower panel). Because we and others have observed that PARP1 is required for MMEJ (Figure 2D, (41)), and assists recruitment of XRCC1 to SSBs (42), we asked if PARP1 regulates XRCC1 recruitment to DSBs. However, the number of XRCC1-γH2AX PLA foci were not reduced in irradiated cells pretreated with PARP1 inhibitor compared to that in control cells (Figure 3B). This strongly suggests that while PARP1 stimulates MMEJ, it is not a rate-limiting factor for XRCC1 recruitment to DSBs, unlike SSB repair (43). Reduced auto-poly(ADP)-ribosylation of PARP1 in rucaparib treated cells confirmed PARP1 inhibition (Figure 3C).

XRCC1's role in DSB repair was further confirmed by the increase in γH2AX foci level and their delayed disappearence in U2OS cells after combined depletion of XRCC1 and DNA-PK inhibition relative to DNA-PK inhibition alone (Figure 3D, E and Supplementary Figure S7). XRCC1-depleted cells also showed higher radiosensitivity than the control cells when treated with the DNA-PK inhibitor (Figure 3F). Together, these data indicate that XRCC1-mediated DSB repair is non-epistatic to NHEJ. This conclusion is further supported by earlier studies showing DSB accumulation in the *Arabidopsis* genome after loss of XRCC1 (44).

### CK2 promotes MMEJ by phosphorylating XRCC1 after irradiation

CK2-catalyzed phosphorylation of XRCC1 promotes SSBR by enhancing its interaction with LIG3 and PNKP (45,46). We tested if enhanced MMEJ activity in irradiated cells is also due to CK2 phosphorylation-dependent protein-protein interactions. FLAG-IP from U2OS cells expressing ectopic XRCC1-FLAG showed a significant increase in CK2α level after irradiation with 3 Gy of X-rays (Figure 4A), consistent with an increase in the number of nuclear PLA foci for XRCC1-CK2α (Figure 4B and Supplementary Figure S13). CK2 activated by stress signaling translocates to the nuclei after irradiation (47), where it colocalizes with the γH2AX foci (48). We observed CK2α localization to the nuclei of irradiated U2OS cells (Figure 4C), together with an increase in phosphorylation of XRCC1 at S518/T519/T523, which was reduced in cells pretreated with the CK2 inhibitor CX-4945 (Figure 4D). The specificity of the phospho-XRCC1 antibody was confirmed by *in vitro* phosphorylation of XRCC1 with recombinant GST-CK2α2 (Supplementary Figure S8). Furthermore, the phospho-XRCC1-γH2AX PLA foci in irradiated cells indicated localization of phosphorylated-XRCC1 at DSBs, which was blocked by CX-4945 (Figure 4E).

### Phosphorylated XRCC1 interacts with the DSB end resection enzymes MRE11 and CtIP after irradiation

The 3′-ssDNA overhang, a prerequisite for stabilizing DSB termini via microhomology-dependent annealing in MMEJ, is generated by the end processing nucleases MRE11 and CtIP (14,49,50); however, their role in coordinating MMEJ is not clearly understood. Because we observed recruitment of XRCC1 at X-ray-induced DSBs, we tested the role of XRCC1 in assembling the MMEJ complex. We isolated IPs of endogenous XRCC1 or XRCC1-FLAG from nuclear extracts of control U2OS cells or those transiently expressing XRCC1-FLAG, and identified MRE11 and CtIP in the IPs (Figure 5A and Supplementary Figure S9A). The levels of these proteins in the IPs increased after irradiation. The XRCC1 level in the U2OS nuclear extract also increased after irradiation (histone H3 was used as the loading control); however, its interaction with MRE11 and CtIP was prevented in cells pretreated with CX-4945, which was further confirmed by PLA analysis (Figure 5A, B and Supplementary Figure S10). We then analyzed FLAG-IP from U2OS nuclear extracts transiently expressing, at a comparable level, $XRCC1^{WT}$- or non-phosphorylable $XRCC1^{CKM}$-FLAG (each of the eight primary serine/threonine CK2 target sites within the linker domain mutated to alanine). We observed a significant increase in MRE11 and CtIP levels in the $XRCC1^{WT}$-FLAG-IP but not in $XRCC1^{CKM}$-FLAG-IP isolated from irradiated cells (Figure 5C, D and Supplementary Figure S11). This confirmed that CK2-mediated phosphorylation of XRCC1 is critical for its interaction with both MRE11 and CtIP. The XRCC1/LIG3 complex has been shown to interact with the MRN complex via the BRCT domain of LIG3 and the FHA domain of NBS1 (9). However, we found that the level of MRE11 in XRCC1-FLAG IP was unaffected by siRNA-mediated depletion of LIG3 or NBS1 (Figure 5E and Supplementary Figure S9B), strongly suggesting direct interaction between XRCC1 and MRE11 rather than indirect association via LIG3–NBS1 interaction.

### CK2-mediated phosphorylation of XRCC1 is required for formation of an MMEJ-competent XRCC1 repair complex

Based on the observation that irradiation enhances the XRCC1-MRE11/CtIP interaction via XRCC1 phosphorylation, we tested if CK2 inhibition or depletion reduces MMEJ activity. Significant reversal of radiation-induced MMEJ in U2OS cells pretreated with CX-4945 or CK2α

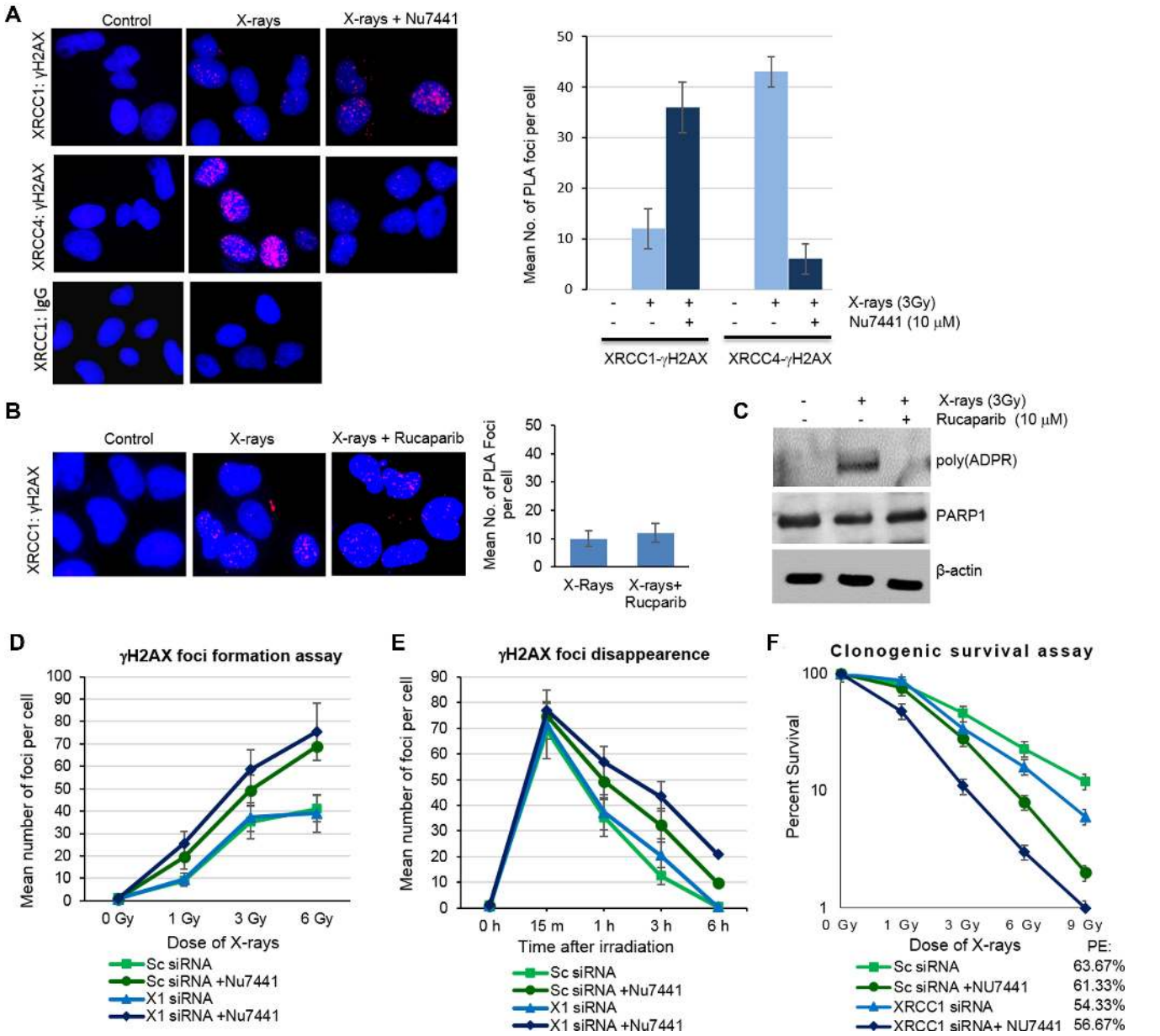


**Figure 3.** XRCC1 is required for repair of X-ray induced DSBs. (**A**) PLA for XRCC1-γH2AX, XRCC4-γH2AX, and XRCC1-IgG interaction in U2OS control cells, and in irradiated cells with or without 10 μM Nu7441. Quantification of the mean number of PLA foci per cell is shown in the right panel. (**B**) PLA for XRCC1-γH2AX interaction in control U2OS cells, and in irradiated cells with or without 10 μM rucaparib. Quantification of the mean number of PLA foci per cell is shown in the right panel. (**C**) Western analysis for poly-ADP-ribosylated (ADPR) PARP1 of cell extracts from U2OS control cells, and irradiated cells with or without 10 μM rucaparib. (**D**) γH2AX immunostaining in U2OS cells transfected with control siRNA or XRCC1 siRNA, with or without NU7441 treatment. Cells were fixed 1 h after irradiation with various doses of X-rays. (**E**) Kinetics of γH2AX foci disappearance in the same set of cells at different time points (15 min, 1, 3, 6 h) following treatment with 3 Gy X-rays. (**F**) Clonogenic survival analysis for the same set of U2OS cells treated with X-rays (0, 1, 3, 6, 9 Gy). Plating efficiency (PE) for each set of cells without irradiation is given.

siRNA (Figure 6A and B) suggests a critical role of CK2-mediated XRCC1 phosphorylation in MMEJ. This was further supported by restoration of radiation-induced enhancement of MMEJ by ectopic WT XRCC1 but not the phosphomutant XRCC1$^{CKM}$ in cells depleted of endogenous XRCC1 (Figure 6C and D), even though the ectopic proteins were similarly localized at the DSB sites (Figure 6E and Supplementary Figure S11).

XRCC1 facilitates formation of multiprotein repair complexes for BER and SSBR by functioning as a scaffold protein (51). Gel filtration analysis of the nuclear extract of irradiated U2OS cells showed that XRCC1 co-eluted with MRE11, NEIL1, and Ku80 in distinct fractions, suggesting that XRCC1 can form distinct multiprotein repair complexes after irradiation (Supplementary Figure S12). Because we detected XRCC1 interaction with the DSB processing nucleases MRE11 and CtIP, we asked if the XRCC1

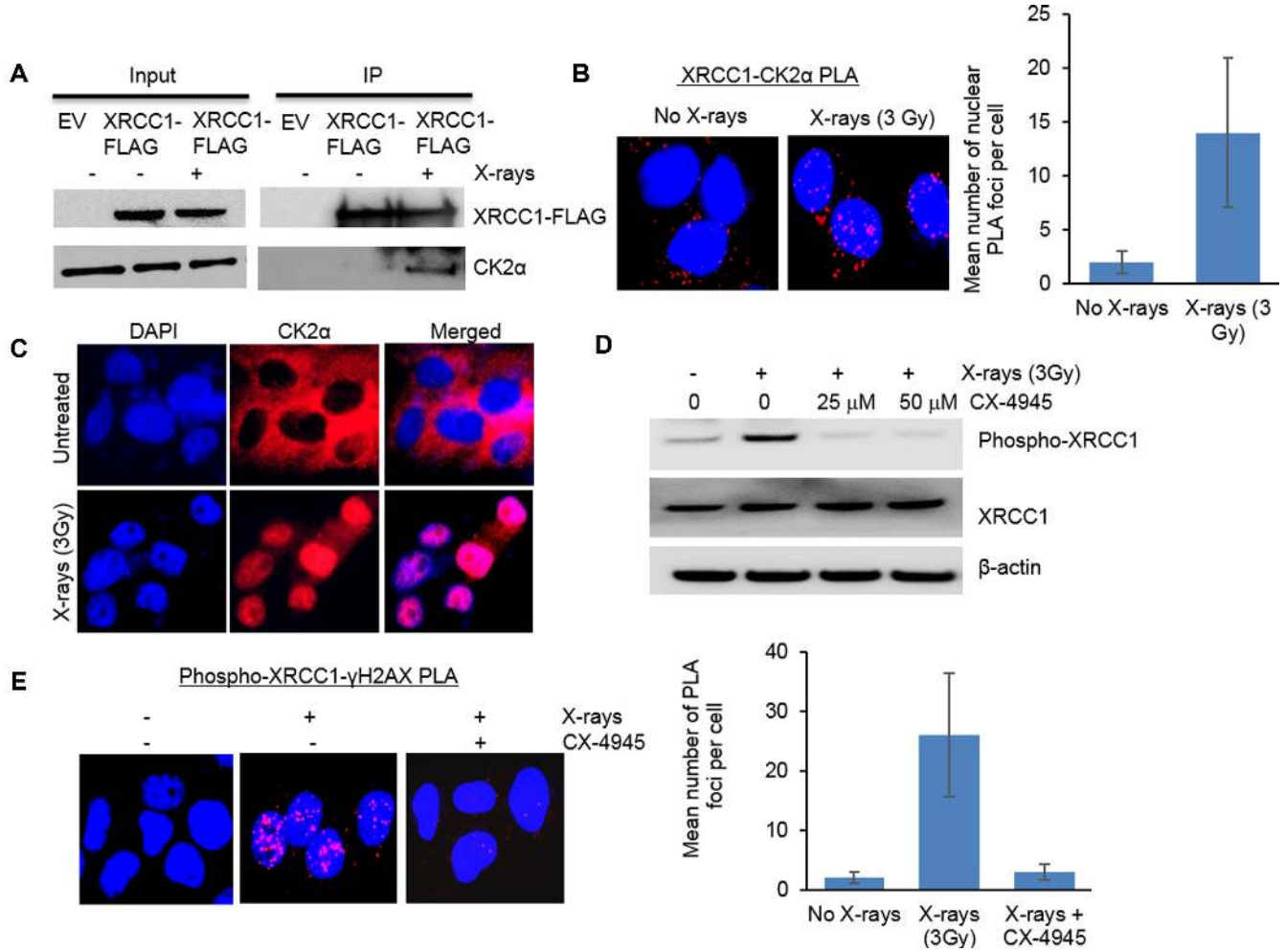


**Figure 4.** CK2 interacts with XRCC1 and phosphorylates it after irradiation. (**A**) Western analysis of CK2α in XRCC1-FLAG IP from nuclear extracts of U2OS cells transiently expressing XRCC1-FLAG, with or without X-ray (3 Gy) treatment. (**B**) PLA for XRCC1-CK2α interaction in untreated and X-ray (3 Gy)-treated U2OS cells. (**C**) CK2α immunostaining in control and irradiated cells. (**D**) Western blot analysis of phosphorylated XRCC1 in U2OS control cells, irradiated cells, and cells treated with CX-4945 (25 μM, 50 μM) prior to irradiation. (**E**) PLA for phospho-XRCC1-γH2AX interaction in control cells, and irradiated cells with or without CX-4945 (50 μM) treatment.

IP could carry out MMEJ *in vitro*. The XRCC1-FLAG IP isolated from the nuclear extract of U2OS cells expressing ectopic XRCC1-FLAG (Figure 7A) was incubated with pNS for 30 minutes at 37°C in a buffer containing ATP and dNTPs, and supplemented with purified recombinant protein complex XRCC1/LIG3α (based on our earlier studies indicating liability of DNA ligases (24)), followed by incubation for 15 h at 16°C (Figure 7A). After transformation, the plasmids recovered from *E. coli* showed that XRCC1-FLAG IP was able to carry out MMEJ *in vitro* with moderate efficiency (Figure 7B, 1st bar). However, unlike plasmids recovered after the *in cell* repair of pNS, which showed both NHEJ and MMEJ products, only MMEJ products were observed for the plasmid substrate repaired *in vitro* with XRCC1 IP. This was expected because the XRCC1 IP should contain only proteins involved in MMEJ/BER, and not in NHEJ. This novel observation provides the first direct evidence for a specific MMEJ protein complex functioning *in cell*, which supports and extends our previous observations for BER (24,52). Irradiation of U2OS cells before isolation of the XRCC1 IP increased its MMEJ activity, consistent with the *in cell* data (Figure 7B, first and second bar). Importantly, pretreatment of the XRCC1-FLAG IP with the MRE11 inhibitors mirin and PFM03 (26) strongly inhibited MMEJ activity, further validating the *in vitro* assay and supporting the functional requirement for both MRE11's exonuclease and endonuclease activities in MMEJ (Figure 7B, fourth and fifth bar). Moreover, pretreatment of cells with CX-4945 prior to isolation of XRCC1 IP reduced the ability of the isolated complex to carry out MMEJ *in vitro* (Figure 7B, third bar). This supports our *in cell* results showing the requirement for CK2-mediated XRCC1 phosphorylation for MMEJ. We further confirmed this by comparing MMEJ activity in FLAG IPs isolated from cells ectopically expressing $XRCC1^{WT}$- or $XRCC1^{CKM}$-FLAG (Figure 7C). Although significantly lower than $XRCC1^{WT}$-IP, $XRCC1^{CKM}$-IP from irradiated cells showed some activity in plasmid circularization, presumably because it partially mimics phosphorylated XRCC1.

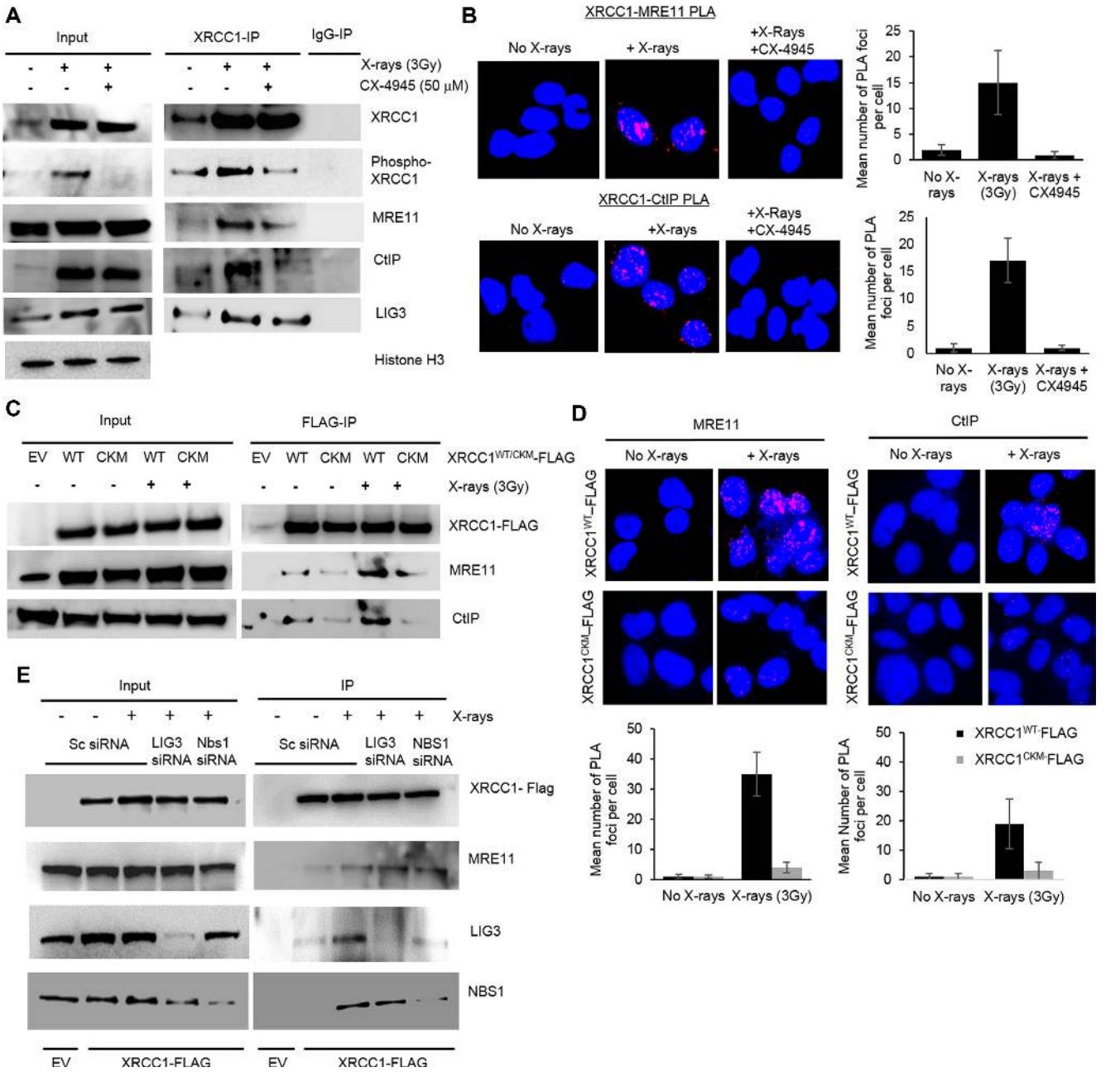


**Figure 5.** XRCC1 phosphorylation by CK2 enhances its interaction with the end resection enzymes MRE11 and CtIP after irradiation. (**A**) Western blot analysis of XRCC1, phospho-XRCC1, MRE11, CtIP, and LIG3 in endogenous XRCC1-IP isolated from nuclear extract of U2OS cells pretreated with X-rays (3 Gy) and/or CX-4945 (50 μM) treatment as indicated. (**B**) PLA for XRCC1-MRE11 (top panel) and XRCC1-CtIP (bottom panel) interactions in U2OS cells with the same treatments. (**C**) Western blot analysis of MRE11 and CtIP in XRCC1$^{WT}$- or XRCC1$^{CKM}$-FLAG IP isolated from nuclear extract of U2OS cells transiently expressing XRCC1$^{WT}$- or XRCC1$^{CKM}$-FLAG. (**D**) PLA for interaction of MRE11 and CtIP with XRCC1$^{WT}$-FLAG (top panels) or XRCC1$^{CKM}$-FLAG (bottom panels) in control or irradiated cells. (**E**) Western blot analysis of MRE11, LIG3 and NBS1 in XRCC1-FLAG IP from control or irradiated U2OS cells transfected with XRCC1-WT-FLAG (48 h), and scrambled (Sc), LIG3, or NBS1 siRNA (100 nM, 72 h), as indicated.

## DISCUSSION

NHEJ, the predominant pathway for DSB repair in the human genome in both growing and quiescent cells, repairs ∼75% of DSBs within 30 min (4). However, DNA breaks with complex damage, such as those induced by IR, require additional processing and may therefore not be repaired via NHEJ (53). For such complex breaks, slower repair processes that involve end trimming, such as accurate HDR or error-prone MMEJ, may be critical. While HDR critically contributes to DSB repair in the replicating cancer cell genome, MMEJ's role in survival of cancer cells is becoming increasingly evident, particularly in cancers with HDR defects (18). Furthermore, MMEJ could be particularly pronounced in DSB repair at repetitive sequences, which are abundant in mammalian genomes (54). Thus, the micro-

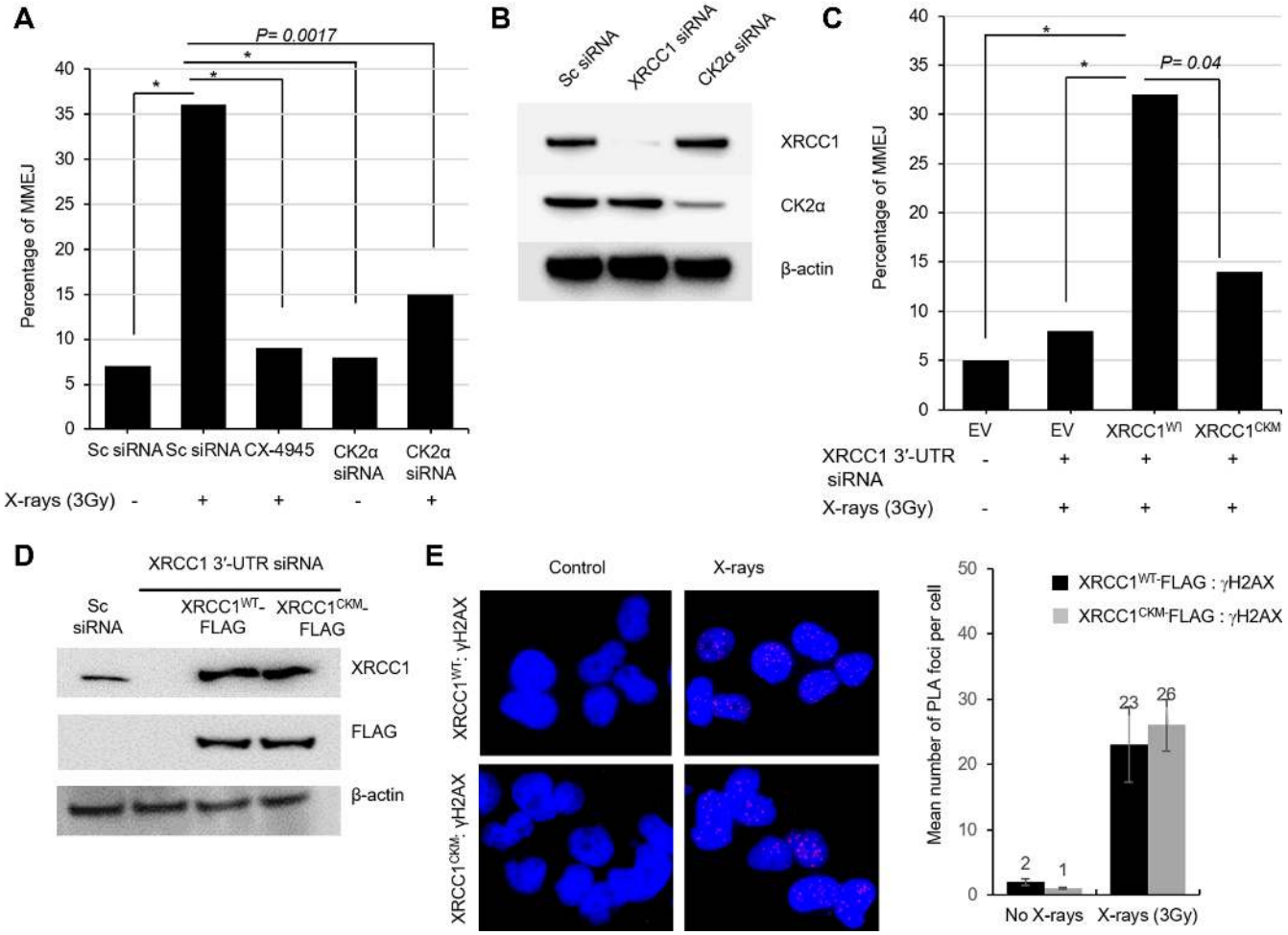


**Figure 6.** CK2 promotes Alt-EJ by phosphorylating XRCC1 following irradiation. (**A**) *In cell* repair of pNS, in control or preirradiated U2OS cells, pretreated wih CX-4945 (25 μM), or CK2 siRNA. (**B**) XRCC1 and CK2α expression in U2OS cells transfected with respective siRNAs (100 nM, 72 h). (**C**) *In cell* repair of pNS in U2OS cells transfected with either empty vector, XRCC1$^{WT}$-FLAG or XRCC1$^{CKM}$-FLAG plasmids, along with either scrambled siRNA or XRCC1 3′-UTR siRNA, as indicated, with/without preirradiation. (**D**) Western analysis for endogenous XRCC1 and ectopic XRCC1$^{WT}$- or XRCC1$^{CKM}$-FLAG after XRCC1 3′-UTR siRNA treatment. (**E**) FLAG-γH2AX PLA in U2OS cells transiently expressing XRCC1$^{WT}$ or XRCC1$^{CKM}$-FLAG in control and irradiated U2OS cells (*P < 0.0001).

homology sequences observed at chromosomal breaks in many cancers implicate MMEJ in DSBR and radioresistance (20,55). In order to unravel the regulation, molecular mechanisms and prevalence of MMEJ, it is important to establish cellular and *in vitro* assays for this 'minor' pathway of DSB repair.

To explore repair of IR-induced DSBs containing 3′-blocked termini (55), we developed a linear plasmid substrate containing 3′-P and DSB-flanking microhomology sequences, and were able to estimate the relative contribution of NHEJ and MMEJ to DSB repair. Although the particular sequence arrangement in this plasmid may not commonly occur in the human genome, it does represent genomic DSBs with microhomology sequences, and thus facilitaes identification of the parameters that regulate MMEJ. In spite of the presence of microhomologies, NHEJ was found to be the preferred pathway of repair in two distinct plasmid substrates in untreated cells, which is in agreement with published reports of the comparatively a minor contribution of MMEJ to DSB repair in normal human cells. At the same time, this provides strong validation for our assay. While our system of repairing naked plasmid DNA does not completely simulate DSB repair at the chromatin level, and cannot exclude possible nonspecific degradation of the DNA substrate during its intracellular transit, it recapitulates the known requirements for NHEJ and MMEJ in mammalian genomes. Thus, this straightforward assay allowed us to identify external factors, such as radiation exposure and signal transduction, that regulate MMEJ. Moreover, our discovery of the ability of XRCC1-IP to carry out MMEJ *in vitro* (in which no possibility of intracellular nonspecific substrate degradation exists) provides an opportunity for establishing biochemical requirements for MMEJ.

During elucidation of BER mechanisms, we and others have documented the formation of dynamic repair complexes that enhance repair of diverse DNA lesions in response to genotoxic stress (52,56,57). It is evident that the formation of such complexes is facilitated by the non-enzymatic scaffold protein XRCC1. The stability of such repair complexes is likely to be dependent on binary in-

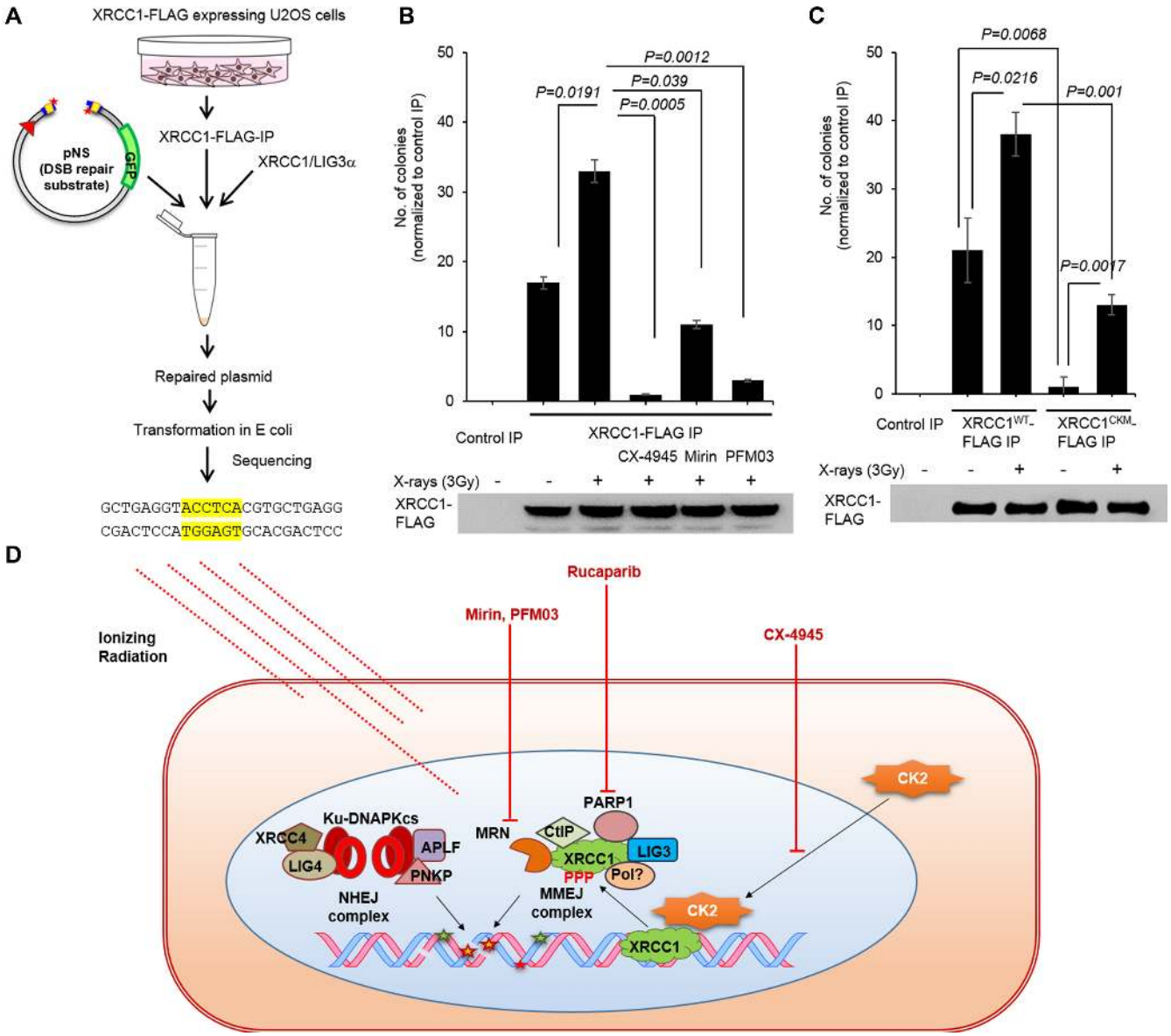


**Figure 7.** Phosphorylation of XRCC1 by CK2 is required for formation of MMEJ proficient repair complex(es). (**A**) Schematic outline of MMEJ assay using XRCC1-FLAG IP. (**B**) Mean number of colonies obtained from the *in vitro* repair assay with empty vector (EV) or XRCC1-FLAG IP from control, irradiated cells and those treated with CX-4945 before irradiation; XRCC1-FLAG IP from irradiated cells was separately incubated with 100 μM mirin or PFM03 before performing *in vitro* repair of pNS. The amount of IP used was normalized to the XRCC1 level. (**C**) *In vitro* repair of pNS with $XRCC1^{WT}$- or $XRCC1^{CKM}$-FLAG IP from control or irradiated cells. Western blot analysis of XRCC1-FLAG levels in the IPs for each experiment are given below. (**D**) Model for CK2 phosphorylation-dependent activation of MMEJ-proficient XRCC1 repair complex: in cancer cells treated with X-rays, CK2 is activated, localizes to the nucleus, phosphorylates XRCC1 bound to chromatin or in the nuclear lamina, and promotes the formation of MMEJ complexes that consist of MRN, CtIP, LIG3 and possibly other MMEJ factors such as DNA polymerases. The active XRCC1 repair complexes then localize to DSB sites (overt or secondarily generated) to carry out MMEJ, possibly competing with or complementing NHEJ. MRE11 endonuclease and exonuclease, PARP1 and CK2 inhibitors prevent activation of MMEJ.

teractions among the components of the complex, which are modulated by their reversible, covalent modifications (58). In delineating the mechanisms of MMEJ, we discovered XRCC1's key role in this repair pathway. Because XRCC1 appears to be limiting in MMEJ, we tested whether radiation-induced covalent modifications of XRCC1 promote its interactions and involvement in MMEJ. XRCC1 is phosphorylated at multiple sites, particularly at the linker regions between the conserved domains (59). Notably, CK2-mediated phosphorylation of XRCC1 at the inter-BRCT domain linker region prevents proteasomal degradation (45), and also reduces its affinity for naked DNA (60). Thus, XRCC1, normally sequestered in chromatin (61), may be mobilized by phosphorylation to form multi-protein repair complexes (Figure 7D), mediated by interactions involving its conserved N-terminal and BRCT domains, as well as the unstructured linker domains (62). The disordered domains in BER-initiating proteins had been

implicated in BER complexes (52,63). Here, we have shown that XRCC1 depends on CK2-mediated phosphorylation for its interaction with MRE11 in irradiated cells, distinct from the interaction between the XRCC1-LIG3 and MRN complexes occurring via LIG3-BRCT and NBS1-FHA domains (9). Our data suggest that phospho-XRCC1 directly interacts with MRE11, which could be further stabilized by LIG3-NBS1 interaction. Hence, it is possible that XRCC1 is recruited at DSBs via MRN rather than PARP1, as is currently believed (15). Future structural studies may illuminate how XRCC1's conformational changes induced by phosphorylation facilitate specific protein-protein interactions. Importantly, we have shown that the induction of XRCC1 repair complexes via IR-induced CK2 phosphorylation could account for the increase in MMEJ-mediated DSBR in irradiated cells. Based on such a scenario, it would be worth investigating how MMEJ is affected by XRCC1 phosphorylation at other sites by CHK2 and DNA-PK (59).

MMEJ, which utilizes the SSBR proteins, is distinct from the HDR and NHEJ pathways for DSB repair. However, several variations of MMEJ likely exist depending on the cell type and the nature of DNA strand breaks. For example, XRCC1 is apparently dispensable for Alt-EJ/MMEJ mediated class-switch recombination or *IgH*/*c-myc* translocation in XRCC4-deficient B cells (64). This is evidently distinct from the MMEJ of IR-induced DSBs. The clustered damage induced by IR in the genome contains a large number of closely spaced bi-stranded lesions that could lead to secondary DSBs formed as BER intermediates (30). These secondary DSBs, possibly with ssDNA overhangs, have poor affinity for Ku, whose binding to the DSB termini is a prerequisite for NHEJ (65,66). Their repair may thus exploit multiple modes of Alt-EJ, including MMEJ, whose initiation is dependent on the recruitment of the SSB factors XRCC1 and PARP1, which compete with Ku (67). Additionally, in the absence of microhomology spanning the DSB, MMEJ could utilize microhomology sequences synthesized *de novo*, for which the required DNA polymerase(s) have not been characterized. Interestingly, treatment of human cells with either glucose oxidase or the radiomimetic drug neocarzinostatin did not result in increased MMEJ as observed in preirradiated cells; although such treatment also caused XRCC1 phosphorylation and its increased interaction with MRE11 (data not shown). One possible explanation for the lack of MMEJ activation in spite of XRCC1 phosphorylation could be the requirement of unknown IR-activated downstream factors or protein modifications, which might uniquely cause MMEJ activation. Furthermore, previous reports on NBS1's role in BER (68) could suggest formation of a discrete XRCC1–MRN complex stimulated by oxidative DNA damage with a role distinct from that in MMEJ.

Another unanswered question that our assay helps address is how resection at the DSB termini regulates MMEJ. Both MMEJ and HDR require generation of 3′ overhangs through resection at the 5′ end. Nonetheless, a profound difference exists between the extended overhang required in HDR versus the short overhang promoting MMEJ. We have shown that MMEJ is dependent on both endo- and 3′→5′ exo-nuclease activities of MRE11, as was also shown in HDR-based DSB repair (26). Furthermore, the endonuclease inhibitor showed a stronger inhibitory effect on MMEJ, suggesting that an initial endonuclease nick followed by exonuclease excision generates the 3′ overhang at blocked DNA breaks in irradiated cells. Overall, the contribution of MRE11, CtIP, EXO1 and DNA2 to excision during DSBR is poorly understood (69). Our results have established a functional role for both nuclease activities of MRE11 in MMEJ. However, extensive end resection by MRE11/CtIP could lead to generation of long ssDNA overhangs where RPA binding would inhibit MMEJ (70). It is therefore important to investigate if XRCC1 regulates end resection at DSBs during MMEJ, similar to the BRCA2 and FANC protein-mediated regulation of MRE11 activity for replication fork protection or inter-strand crosslink repair (71,72).

In summary, we have shown that the contribution of MMEJ to DSB repair in the genome is affected by radiation exposure via enhancement of the formation of MMEJ-proficient XRCC1 complex(es). Paradoxically, radiation therapy, while killing tumor cells, may induce radioresistance in surviving cells by activating MMEJ to repair radiation-induced genome damage, possibly leading to increased mutations. It is possible that the altered phenotype caused by some of these mutations provides growth advantage to the surviving cells and may promote tumor regrowth. Our results showing that XRCC1-MRE11 interaction, dependent on XRCC1 phosphorylation by CK2, activates MMEJ suggest that this interaction could be a potential therapeutic target for inhibiting MMEJ, thereby increasing radiosensitivity of cancer cells.

## SUPPLEMENTARY DATA

Supplementary Data are available at NAR online.

## ACKNOWLEDGEMENTS

We thank Dr K. Caldecott (University of Sussex, UK) for the gift of the XRCC1 plasmids, XH-pCD2E ($XRCC1^{WT}$) and XHCKM-pCD2E ($XRCC1^{CKM}$), and Dr T.K. Pandita (Houston Methodist Research Institute) for access to the X-ray source. We thank Dr David Haviland of the ACTM core facility at HMRI for providing assistance with performing FACS.

## FUNDING

The work was supported in part by USPHS grants R01 CA158910, and R01 GM105090 (to S.M.), R01 NS088645 (to M.L.H.), P01 CA92548 (to J.A.T. and S.M.), R01 CA117638, and also Robert A Welch Chemistry Chair, Cancer Prevention and Research Institute of Texas, and University of Texas System Science and Technology Acquisition and Retention Program (to J.A.T.), National Space Biomedical Research Institute NCC 9-58 (to B.E.), and Biochemistry & Molecular Biology Graduate Program at UTMB, Galveston, TX (to A.D.).
*Conflict of interest statement.* None declared.

## REFERENCES


1. Begg,A.C., Stewart,F.A. and Vens,C. (2011) Strategies to improve radiotherapy with targeted drugs. *Nat. Rev. Cancer*, **11**, 239–253.
2. Sutherland,B.M., Bennett,P.V., Sidorkina,O. and Laval,J. (2000) Clustered DNA damages induced in isolated DNA and in human cells by low doses of ionizing radiation. *Proc. Natl. Acad. Sci. U.S.A.*, **97**, 103–108.
3. Jeggo,P.A., Geuting,V. and Lobrich,M. (2011) The role of homologous recombination in radiation-induced double-strand break repair. *Radiother. Oncol.*, **101**, 7–12.
4. Davis,A.J. and Chen,D.J. (2013) DNA double strand break repair via non-homologous end-joining. *Transl. Cancer Res.*, **2**, 130–143.
5. Schipler,A. and Iliakis,G. (2013) DNA double-strand-break complexity levels and their possible contributions to the probability for error-prone processing and repair pathway choice. *Nucleic Acids Res.*, **41**, 7589–7605.
6. Betermier,M., Bertrand,P. and Lopez,B.S. (2014) Is non-homologous end-joining really an inherently error-prone process? *PLoS Genet*, **10**, e1004086.
7. Mimitou,E.P. and Symington,L.S. (2010) Ku prevents Exo1 and Sgs1-dependent resection of DNA ends in the absence of a functional MRX complex or Sae2. *EMBO J.*, **29**, 3358–3369.
8. Sharma,S., Javadekar,S.M., Pandey,M., Srivastava,M., Kumari,R. and Raghavan,S.C. (2015) Homology and enzymatic requirements of microhomology-dependent alternative end joining. *Cell Death Dis.*, **6**, e1697.
9. Della-Maria,J., Zhou,Y., Tsai,M.S., Kuhnlein,J., Carney,J.P., Paull,T.T. and Tomkinson,A.E. (2011) Human Mre11/human Rad50/Nbs1 and DNA ligase IIIalpha/XRCC1 protein complexes act together in an alternative nonhomologous end joining pathway. *J. Biol. Chem.*, **286**, 33845–33853.
10. Lu,G., Duan,J., Shu,S., Wang,X., Gao,L., Guo,J. and Zhang,Y. (2016) Ligase I and ligase III mediate the DNA double-strand break ligation in alternative end-joining. *Proc. Natl. Acad. Sci. U.S.A.*, **113**, 1256–1260.
11. McVey,M. and Lee,S.E. (2008) MMEJ repair of double-strand breaks (director's cut): deleted sequences and alternative endings. *Trends Genet.*, **24**, 529–538.
12. Audebert,M., Salles,B., Weinfeld,M. and Calsou,P. (2006) Involvement of polynucleotide kinase in a poly(ADP-ribose) polymerase-1-dependent DNA double-strand breaks rejoining pathway. *J. Mol. Biol.*, **356**, 257–265.
13. Mansour,W.Y., Rhein,T. and Dahm-Daphi,J. (2010) The alternative end-joining pathway for repair of DNA double-strand breaks requires PARP1 but is not dependent upon microhomologies. *Nucleic Acids Res.*, **38**, 6065–6077.
14. Truong,L.N., Li,Y., Shi,L.Z., Hwang,P.Y., He,J., Wang,H., Razavian,N., Berns,M.W. and Wu,X. (2013) Microhomology-mediated End Joining and Homologous Recombination share the initial end resection step to repair DNA double-strand breaks in mammalian cells. *Proc. Natl. Acad. Sci. U.S.A.*, **110**, 7720–7725.
15. Frit,P., Barboule,N., Yuan,Y., Gomez,D. and Calsou,P. (2014) Alternative end-joining pathway(s): bricolage at DNA breaks. *DNA Repair (Amst.)*, **17**, 81–97.
16. Wu,W., Wang,M., Wu,W., Singh,S.K., Mussfeldt,T. and Iliakis,G. (2008) Repair of radiation induced DNA double strand breaks by backup NHEJ is enhanced in G2. *DNA Repair (Amst.)*, **7**, 329–338.
17. Sfeir,A. and Symington,L.S. (2015) Microhomology-mediated end joining: A back-up survival mechanism or dedicated pathway? *Trends Biochem. Sci.*, **40**, 701–714.
18. Ceccaldi,R., Liu,J.C., Amunugama,R., Hajdu,I., Primack,B., Petalcorin,M.I., O'Connor,K.W., Konstantinopoulos,P.A., Elledge,S.J., Boulton,S.J. *et al.* (2015) Homologous-recombination-deficient tumours are dependent on Poltheta-mediated repair. *Nature*, **518**, 258–262.
19. Yang,L., Luquette,L.J., Gehlenborg,N., Xi,R., Haseley,P.S., Hsieh,C.H., Zhang,C., Ren,X., Protopopov,A., Chin,L. *et al.* (2013) Diverse mechanisms of somatic structural variations in human cancer genomes. *Cell*, **153**, 919–929.
20. Mattarucchi,E., Guerini,V., Rambaldi,A., Campiotti,L., Venco,A., Pasquali,F., Lo Curto,F. and Porta,G. (2008) Microhomologies and interspersed repeat elements at genomic breakpoints in chronic myeloid leukemia. *Genes Chromosomes Cancer*, **47**, 625–632.
21. Henner,W.D., Rodriguez,L.O., Hecht,S.M. and Haseltine,W.A. (1983) gamma Ray induced deoxyribonucleic acid strand breaks. 3′ Glycolate termini. *J. Biol. Chem.*, **258**, 711–713.
22. Povirk,L.F. (2012) Processing of damaged DNA ends for double-strand break repair in mammalian cells. *ISRN Mol. Biol.*, **2012**, doi:10.5402/2012/345805.
23. Buchko,G.W. and Weinfeld,M. (1993) Influence of nitrogen, oxygen, and nitroimidazole radiosensitizers on DNA damage induced by ionizing radiation. *Biochemistry*, **32**, 2186–2193.
24. Hegde,M.L., Hegde,P.M., Bellot,L.J., Mandal,S.M., Hazra,T.K., Li,G.M., Boldogh,I., Tomkinson,A.E. and Mitra,S. (2013) Prereplicative repair of oxidized bases in the human genome is mediated by NEIL1 DNA glycosylase together with replication proteins. *Proc. Natl. Acad. Sci. U.S.A.*, **110**, E3090–E3099.
25. Rasouli-Nia,A., Karimi-Busheri,F. and Weinfeld,M. (2004) Stable down-regulation of human polynucleotide kinase enhances spontaneous mutation frequency and sensitizes cells to genotoxic agents. *Proc. Natl. Acad. Sci. U.S.A.*, **101**, 6905–6910.
26. Shibata,A., Moiani,D., Arvai,A.S., Perry,J., Harding,S.M., Genois,M.M., Maity,R., van Rossum-Fikkert,S., Kertokalio,A., Romoli,F. *et al.* (2014) DNA double-strand break repair pathway choice is directed by distinct MRE11 nuclease activities. *Mol. Cell*, **53**, 7–18.
27. Lee,Y.S. and Chung,M.H. (2003) Base excision repair synthesis of DNA containing 8-oxoguanine in Escherichia coli. *Exp. Mol. Med.*, **35**, 106–112.
28. Ziegler,K., Bui,T., Frisque,R.J., Grandinetti,A. and Nerurkar,V.R. (2004) A rapid in vitro polyomavirus DNA replication assay. *J. Virol. Methods*, **122**, 123–127.
29. Gunn,A. and Stark,J.M. (2012) I-SceI-based assays to examine distinct repair outcomes of mammalian chromosomal double strand breaks. *Methods Mol. Biol.*, **920**, 379–391.
30. Lomax,M.E., Folkes,L.K. and O'Neill,P. (2013) Biological consequences of radiation-induced DNA damage: relevance to radiotherapy. *Clin. Oncol. (R. Coll. Radiol.)*, **25**, 578–585.
31. Prell,A. and Wackernagel,W. (1980) Degradation of linear and circular DNA with gaps by the recBC enzyme of Escherichia coli. Effects of gap length and the presence of cell-free extracts. *Eur. J. Biochem.*, **105**, 109–116.
32. Decottignies,A. (2007) Microhomology-mediated end joining in fission yeast is repressed by pku70 and relies on genes involved in homologous recombination. *Genetics*, **176**, 1403–1415.
33. Yu,A.M. and McVey,M. (2010) Synthesis-dependent microhomology-mediated end joining accounts for multiple types of repair junctions. *Nucleic Acids Res.*, **38**, 5706–5717.
34. Chappell,C., Hanakahi,L.A., Karimi-Busheri,F., Weinfeld,M. and West,S.C. (2002) Involvement of human polynucleotide kinase in double-strand break repair by non-homologous end joining. *EMBO J.*, **21**, 2827–2832.
35. Weinfeld,M., Mani,R.S., Abdou,I., Aceytuno,R.D. and Glover,J.N. (2011) Tidying up loose ends: the role of polynucleotide kinase/phosphatase in DNA strand break repair. *Trends Biochem. Sci.*, **36**, 262–271.
36. Scuric,Z., Chan,C.Y., Hafer,K. and Schiestl,R.H. (2009) Ionizing radiation induces microhomology-mediated end joining in trans in yeast and mammalian cells. *Radiat. Res.*, **171**, 454–463.
37. Soni,A., Siemann,M., Pantelias,G.E. and Iliakis,G. (2015) Marked contribution of alternative end-joining to chromosome-translocation-formation by stochastically induced DNA double-strand-breaks in G2-phase human cells. *Mutat. Res. Genet. Toxicol. Environ. Mutagen.*, **793**, 2–8.
38. Wang,H., Perrault,A.R., Takeda,Y., Qin,W., Wang,H. and Iliakis,G. (2003) Biochemical evidence for Ku-independent backup pathways of NHEJ. *Nucleic Acids Res.*, **31**, 5377–5388.
39. Xu,B., Kim,S.T., Lim,D.S. and Kastan,M.B. (2002) Two molecularly distinct G(2)/M checkpoints are induced by ionizing irradiation. *Mol. Cell. Biol.*, **22**, 1049–1059.
40. Saribasak,H., Maul,R.W., Cao,Z., McClure,R.L., Yang,W., McNeill,D.R., Wilson,D.M. 3rd and Gearhart,P.J. (2011) XRCC1 suppresses somatic hypermutation and promotes alternative nonhomologous end joining in Igh genes. *J. Exp. Med.*, **208**, 2209–2216.

41. Audebert,M., Salles,B. and Calsou,P. (2004) Involvement of poly(ADP-ribose) polymerase-1 and XRCC1/DNA ligase III in an alternative route for DNA double-strand breaks rejoining. *J. Biol. Chem.*, **279**, 55117–55126.
42. Wei,L., Nakajima,S., Hsieh,C.L., Kanno,S., Masutani,M., Levine,A.S., Yasui,A. and Lan,L. (2013) Damage response of XRCC1 at sites of DNA single strand breaks is regulated by phosphorylation and ubiquitylation after degradation of poly(ADP-ribose). *J. Cell Sci.*, **126**, 4414–4423.
43. Abdou,I., Poirier,G.G., Hendzel,M.J. and Weinfeld,M. (2015) DNA ligase III acts as a DNA strand break sensor in the cellular orchestration of DNA strand break repair. *Nucleic Acids Res.*, **43**, 875–892.
44. Charbonnel,C., Gallego,M.E. and White,C.I. (2010) Xrcc1-dependent and Ku-dependent DNA double-strand break repair kinetics in Arabidopsis plants. *Plant J.*, **64**, 280–290.
45. Parsons,J.L., Dianova,II, Finch,D., Tait,P.S., Strom,C.E., Helleday,T. and Dianov,G.L. (2010) XRCC1 phosphorylation by CK2 is required for its stability and efficient DNA repair. *DNA Repair (Amst.)*, **9**, 835–841.
46. Loizou,J.I., El-Khamisy,S.F., Zlatanou,A., Moore,D.J., Chan,D.W., Qin,J., Sarno,S., Meggio,F., Pinna,L.A. and Caldecott,K.W. (2004) The protein kinase CK2 facilitates repair of chromosomal DNA single-strand breaks. *Cell*, **117**, 17–28.
47. Yamane,K. and Kinsella,T.J. (2005) CK2 inhibits apoptosis and changes its cellular localization following ionizing radiation. *Cancer Res.*, **65**, 4362–4367.
48. Olsen,B.B., Wang,S.Y., Svenstrup,T.H., Chen,B.P. and Guerra,B. (2012) Protein kinase CK2 localizes to sites of DNA double-strand break regulating the cellular response to DNA damage. *BMC Mol. Biol.*, **13**, 7.
49. Xie,A., Kwok,A. and Scully,R. (2009) Role of mammalian Mre11 in classical and alternative nonhomologous end joining. *Nat. Struct. Mol. Biol.*, **16**, 814–818.
50. Lee-Theilen,M., Matthews,A.J., Kelly,D., Zheng,S. and Chaudhuri,J. (2011) CtIP promotes microhomology-mediated alternative end joining during class-switch recombination. *Nat. Struct. Mol. Biol.*, **18**, 75–79.
51. Hanssen-Bauer,A., Solvang-Garten,K., Akbari,M. and Otterlei,M. (2012) X-ray repair cross complementing protein 1 in base excision repair. *Int. J. Mol. Sci.*, **13**, 17210–17229.
52. Hegde,P.M., Dutta,A., Sengupta,S., Mitra,J., Adhikari,S., Tomkinson,A.E., Li,G.M., Boldogh,I., Hazra,T.K., Mitra,S. *et al.* (2015) The C-terminal domain (CTD) of human DNA glycosylase NEIL1 is required for forming BERosome repair complex with DNA replication proteins at the replicating genome: dominant negative function of the CTD. *Biol. Chem.*, **290**, 20919–20933.
53. Averbeck,N.B., Ringel,O., Herrlitz,M., Jakob,B., Durante,M. and Taucher-Scholz,G. (2014) DNA end resection is needed for the repair of complex lesions in G1-phase human cells. *Cell Cycle*, **13**, 2509–2516.
54. Villarreal,D.D., Lee,K., Deem,A., Shim,E.Y., Malkova,A. and Lee,S.E. (2012) Microhomology directs diverse DNA break repair pathways and chromosomal translocations. *PLoS Genet.*, **8**, e1003026.
55. Singleton,B.K., Griffin,C.S. and Thacker,J. (2002) Clustered DNA damage leads to complex genetic changes in irradiated human cells. *Cancer Res.*, **62**, 6263–6269.
56. Luijsterburg,M.S., von Bornstaedt,G., Gourdin,A.M., Politi,A.Z., Mone,M.J., Warmerdam,D.O., Goedhart,J., Vermeulen,W., van Driel,R. and Hofer,T. (2010) Stochastic and reversible assembly of a multiprotein DNA repair complex ensures accurate target site recognition and efficient repair. *J. Cell Biol.*, **189**, 445–463.
57. Raschle,M., Smeenk,G., Hansen,R.K., Temu,T., Oka,Y., Hein,M.Y., Nagaraj,N., Long,D.T., Walter,J.C., Hofmann,K. *et al.* (2015) DNA repair. Proteomics reveals dynamic assembly of repair complexes during bypass of DNA cross-links. *Science*, **348**, 1253671.
58. Polo,S.E. and Jackson,S.P. (2011) Dynamics of DNA damage response proteins at DNA breaks: a focus on protein modifications. *Genes Dev.*, **25**, 409–433.
59. London,R.E. (2015) The structural basis of XRCC1-mediated DNA repair. *DNA Repair (Amst.)*, **30**, 90–103.
60. Strom,C.E., Mortusewicz,O., Finch,D., Parsons,J.L., Lagerqvist,A., Johansson,F., Schultz,N., Erixon,K., Dianov,G.L. and Helleday,T. (2011) CK2 phosphorylation of XRCC1 facilitates dissociation from DNA and single-strand break formation during base excision repair. *DNA Repair (Amst.)*, **10**, 961–969.
61. Kubota,Y., Takanami,T., Higashitani,A. and Horiuchi,S. (2009) Localization of X-ray cross complementing gene 1 protein in the nuclear matrix is controlled by casein kinase II-dependent phosphorylation in response to oxidative damage. *DNA Repair (Amst.)*, **8**, 953–960.
62. Dutta,A., Yang,C., Sengupta,S., Mitra,S. and Hegde,M.L. (2015) New paradigms in the repair of oxidative damage in human genome: mechanisms ensuring repair of mutagenic base lesions during replication and involvement of accessory proteins. *Cell. Mol. Life Sci.*, **72**, 1679–1698.
63. Fong,J.H., Shoemaker,B.A., Garbuzynskiy,S.O., Lobanov,M.Y., Galzitskaya,O.V. and Panchenko,A.R. (2009) Intrinsic disorder in protein interactions: insights from a comprehensive structural analysis. *PLoS Comput. Biol.*, **5**, e1000316.
64. Boboila,C., Oksenych,V., Gostissa,M., Wang,J.H., Zha,S., Zhang,Y., Chai,H., Lee,C.S., Jankovic,M., Saez,L.M. *et al.* (2012) Robust chromosomal DNA repair via alternative end-joining in the absence of X-ray repair cross-complementing protein 1 (XRCC1). *Proc. Natl. Acad. Sci. U.S.A.*, **109**, 2473–2478.
65. Ristic,D., Modesti,M., Kanaar,R. and Wyman,C. (2003) Rad52 and Ku bind to different DNA structures produced early in double-strand break repair. *Nucleic Acids Res.*, **31**, 5229–5237.
66. Daley,J.M. and Wilson,T.E. (2005) Rejoining of DNA double-strand breaks as a function of overhang length. *Mol. Cell. Biol.*, **25**, 896–906.
67. Wang,M., Wu,W., Wu,W., Rosidi,B., Zhang,L., Wang,H. and Iliakis,G. (2006) PARP-1 and Ku compete for repair of DNA double strand breaks by distinct NHEJ pathways. *Nucleic Acids Res.*, **34**, 6170–6182.
68. Sagan,D., Muller,R., Kroger,C., Hematulin,A., Mortl,S. and Eckardt-Schupp,F. (2009) The DNA repair protein NBS1 influences the base excision repair pathway. *Carcinogenesis*, **30**, 408–415.
69. Hoa,N.N., Akagawa,R., Yamasaki,T., Hirota,K., Sasa,K., Natsume,T., Kobayashi,J., Sakuma,T., Yamamoto,T., Komatsu,K. *et al.* (2015) Relative contribution of four nucleases, CtIP, Dna2, Exo1 and Mre11, to the initial step of DNA double-strand break repair by homologous recombination in both the chicken DT40 and human TK6 cell lines. *Genes Cells*, **20**, 1059–1076.
70. Deng,S.K., Gibb,B., de Almeida,M.J., Greene,E.C. and Symington,L.S. (2014) RPA antagonizes microhomology-mediated repair of DNA double-strand breaks. *Nat. Struct. Mol. Biol.*, **21**, 405–412.
71. Schlacher,K., Wu,H. and Jasin,M. (2012) A distinct replication fork protection pathway connects Fanconi anemia tumor suppressors to RAD51-BRCA1/2. *Cancer Cell*, **22**, 106–116.
72. Suhasini,A.N., Sommers,J.A., Muniandy,P.A., Coulombe,Y., Cantor,S.B., Masson,J.Y., Seidman,M.M. and Brosh,R.M. Jr2013) Fanconi anemia group J helicase and MRE11 nuclease interact to facilitate the DNA damage response. *Mol. Cell. Biol.*, **33**, 2212–2227.